Daneshjou et al., http://www.jcb.org/cgi/content/full/jcb.201409108/DC1

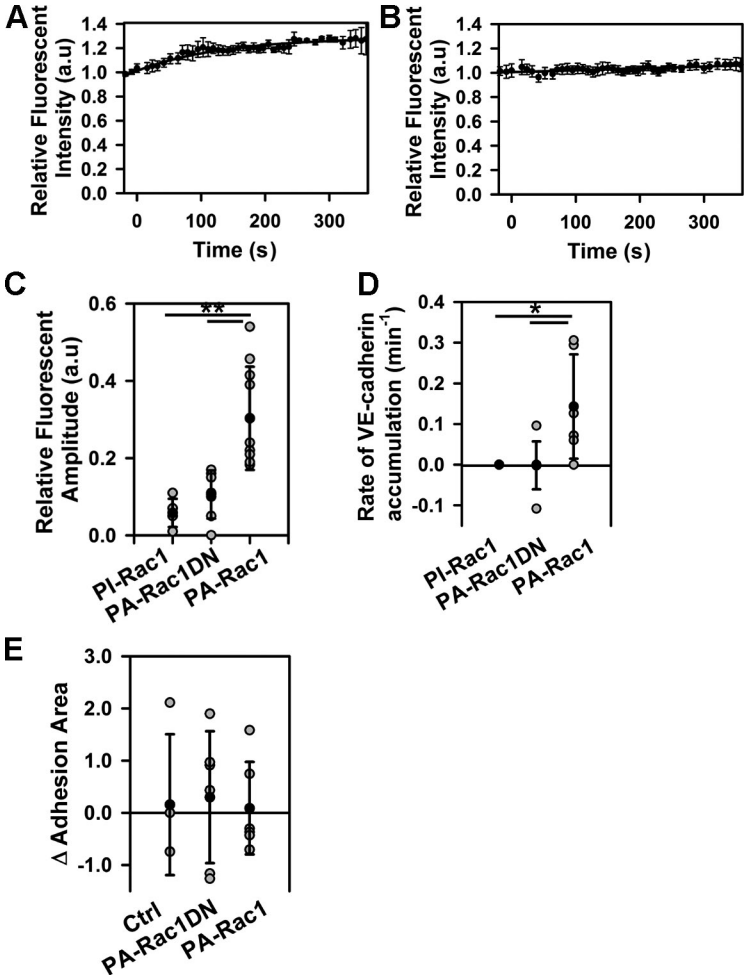


Figure S1. **Activation of PA-Rac1 increases VE-cadherin density without affecting the area of adhesion zone.** (A and B) Relative changes in VE-cadherin–GFP fluorescent intensity after activation of PA-Rac1 (A) or PA-Rac1DN (B) in HMECs. Analyses are performed as in Fig.1; means ± SEM, *n* = 8–10. (C) Amplitude of VE-cadherin–GFP accumulation after activation of PI-Rac1 (0.06 ± 0.04), PA-Rac1DN (0.11 ± 0.06), or PA-Rac1 (0.30 ± 0.13); means ± SD, *n* = 5–10; **, P < 0.005. (D) Rate constant for VE-cadherin–GFP accumulation after activation of PA-Rac1 was 0.14 ± 0.13 $min^{-1}$, whereas no significant changes were observed after activation of PI-Rac1 or PA-Rac1DN; means ± SD, *n* = 5–8; *, P < 0.05. (E) Changes in VE-cadherin adhesion area within irradiation zone after activation of PA-Rac1 or PA-Rac1DN and in adjacent cells (Ctrl, control). Means ± SD, *n* = 4–6. a.u., arbitrary unit.

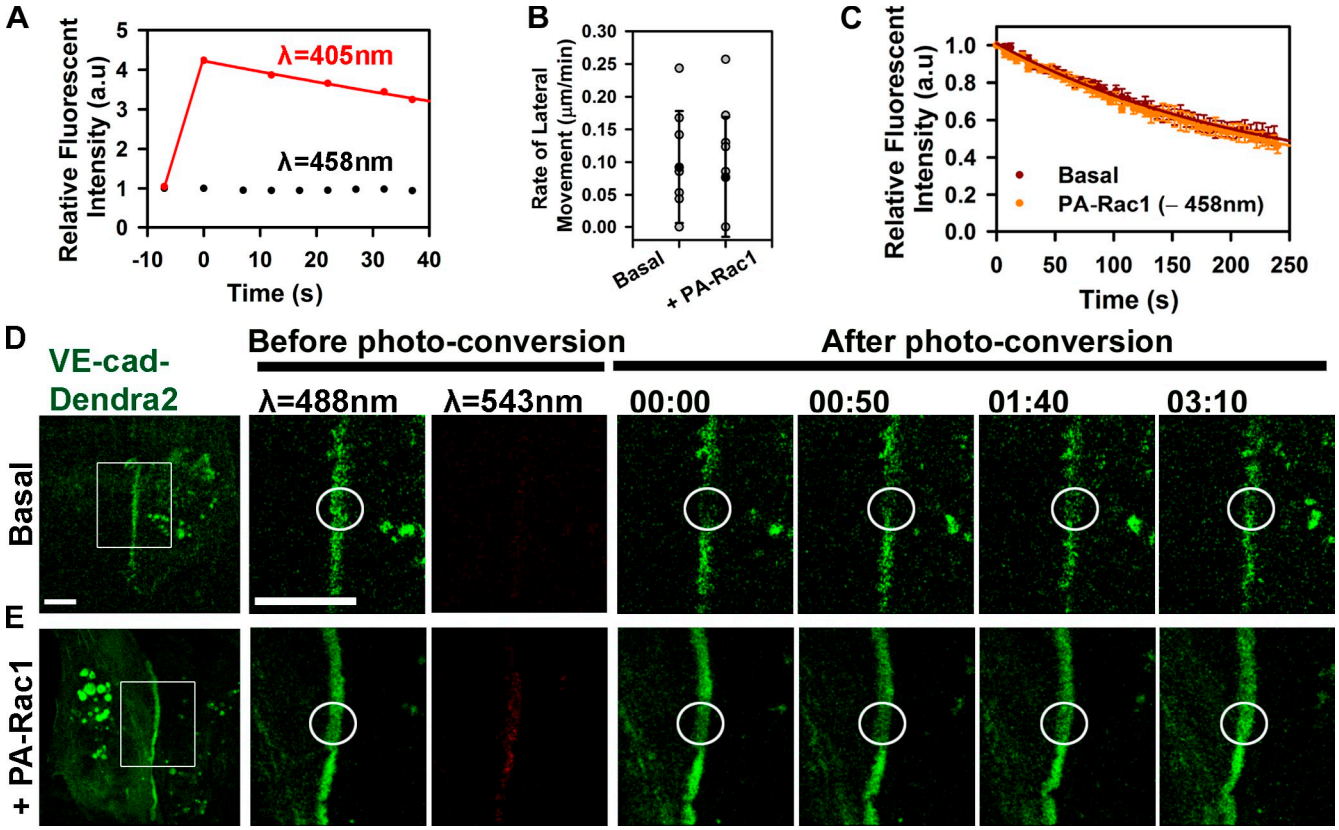


Figure S2. **Effects of Rac1 on VE-cadherin kinetics.** (A) Changes in fluorescent emission at 543 nm after irradiation of VE-cadherin–Dendra2 with λ = 405-nm and λ = 458-nm laser beams at time 0. Representative tracers from reproducible datasets of *n* = 7 and 3, respectively. (B) Rate of lateral movement of VE-cadherin–Dendra2 for basal condition (0.09 ± 0.09 μm/min) and after PA-Rac1 activation (0.08 ± 0.09 μm/min); means ± SD; *n* = 8–10. (C) Cells were transfected with VE-cadherin–Dendra2 alone or with PA-Rac1. Changes in relative fluorescent intensity of VE-cadherin–Dendra2 were monitored after Dendra2 photoconversion; no PA-Rac1 activation was performed; means ± SEM, *n* = 3 and 7. (D and E) Time-lapse images of VE-cadherin–Dendra2 (VE-cad-Dendra2) emission at 488 nm before and after photoconversion within the circular region under basal condition (D) and after activation of PA-Rac1 (E). Boxes are magnified on the right. Time is given in minutes and seconds. Bars, 10 μm. a.u., arbitrary unit.

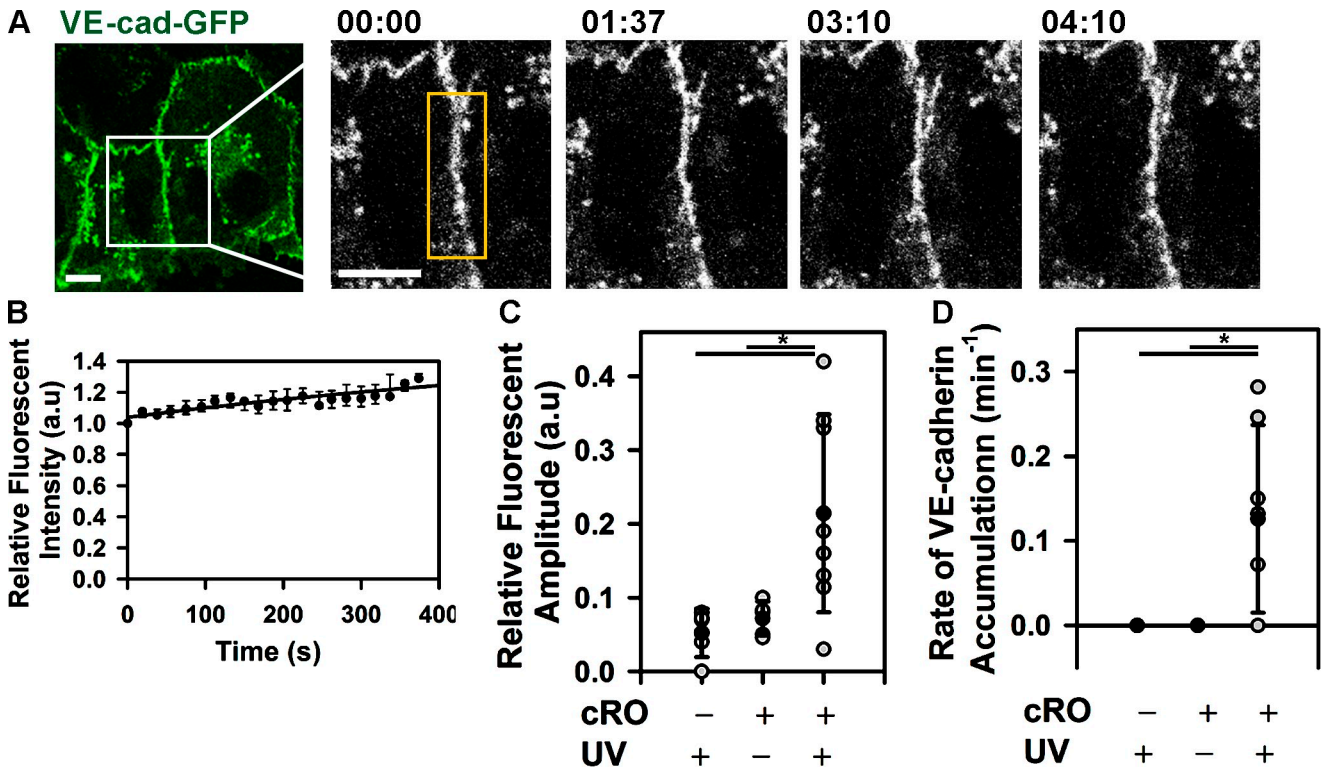


Figure S3. **Spatial inhibition of ROCK at AJs increases VE-cadherin density.** (A) Time-lapse images of VE-cadherin–GFP (VE-cad-GFP) before and after cRO uncaging within the rectangular region at time 0. Bars, 10 µm. (B) Relative changes in VE-cadherin–GFP fluorescent intensity at AJs after cRO uncaging fitted to an exponential rise; means ± SEM, $n = 8$. (C) Amplitude of VE-cadherin–GFP accumulation at AJs in cells irradiated with 405 nm (0.05 ± 0.03) or treated with cRO without (0.07 ± 0.02) and with uncaging (0.21 ± 0.13); means ± SD, $n = 5–8$; *, $P < 0.05$. (D) Rate constant for VE-cadherin–GFP accumulation after cRO uncaging was 0.13 ± 0.11 $min^{-1}$, whereas no significant changes were observed in cells irradiated with a 405-nm laser beam or cells treated with caged cRO; $n = 5–7$; *, $P < 0.05$. a.u., arbitrary unit.